

Issues in the Wavelength-Dispersive Spectrometric Characterization of $\text{YBa}_2\text{Cu}_3\text{O}_{7-\delta}$

Karoline Müller, Andrea L. Baker, James K. Meen, Minsoo Kim, Han Ju Lee, Eduard Galstyan, Herbert Freyhardt, and T. Randall Lee

Abstract— $\text{YBa}_2\text{Cu}_3\text{O}_{7-\delta}$ (Y123) can have significant variation in oxygen content on a micron scale in superconducting devices, and this causes a range of superconducting properties—generally impairing the performance of the superconductor. This study initially aimed to determine variation in O content of Y123 using electron microprobe analysis. High-quality electron microprobe analysis requires flat, usually polished, samples. Polishing Y123 produces a change in O content in surface layers relative to that of the parent as polishing a ceramic involves partial to complete surface amorphization. The analyses are not appropriate for the parent (much lower O), evidence of inhomogeneity of oxygen is removed, and the resultant material absorbs oxygen from the environment. After ion milling, the new surface more reflects the parent; comparison of unprocessed materials with polished and milled ones suggests that milling does not seriously alter the O K α peak shape. Furthermore, milled surfaces reveal inhomogeneities obscured in polished surfaces. O K α peaks derived from milled surfaces were compared with those from standard oxides; all standards were found to have peak shapes that do not conform to those of Y123. Because peak width:height is markedly different, the analytical assumption that peak height is proportional to peak area is violated. Alternative methods of determining peak area without mapping the entire peak are required to perform high-quality Y123 analyses; these are being developed.

Index Terms—Chemical analysis, electron beams, electron microscopy, high-temperature superconductors.

I. INTRODUCTION

ANALYSIS of $\text{YBa}_2\text{Cu}_3\text{O}_{7-\delta}$ (Y123) poses several unusual challenges. This paper concentrates on our work in developing the techniques to produce high-quality analyses of oxygen in Y123 by electron microprobe analyzer (EMPA)

Manuscript received October 5, 2012; accepted January 14, 2013. Date of publication February 4, 2013; date of current version March 8, 2013. J. K. Meen was supported by the State of Texas through Grants through TcSUH. T. R. Lee was supported by the Robert A. Welch Foundation (Grant E-1320) and TcSUH.

K. Müller and E. Galstyan are with the Texas Center for Superconductivity at University of Houston (TcSUH), Houston, TX 77204 USA (e-mail: kmueller@uh.edu; egalstyan@uh.edu).

A. L. Baker is with the Department of Biomedical Engineering, Texas A&M University, College Station, TX 77843 USA (e-mail: abaker21@neo.tamu.edu).

J. K. Meen and T. R. Lee are with the Texas Center for Superconductivity at University of Houston, Houston, TX 77204 USA. They are also with the Department of Chemistry, University of Houston, Houston, TX 77204 USA (e-mail: jmeen@uh.edu; trlee@uh.edu).

M. Kim is with Materials Science and Engineering, University of Delaware, Newark, DE 19716 USA (e-mail: minsoo94@gmail.com).

H. Ju Lee is with the Department of Chemistry, University of Houston, Houston, TX 77204 USA (e-mail: hanju.lee73@gmail.com).

H. Freyhardt is with the Texas Center for Superconductivity at University of Houston. He is also with the Department of Mechanical Engineering, University of Houston, Houston, TX 77204 USA (e-mail: hcfreyha@Central.UH.EDU).

Digital Object Identifier 10.1109/TASC.2013.2242111

using wavelength-dispersive x-ray spectrometric (WDS) analysis. Application of these techniques to Y123 requires rather different approaches from those used for most ceramics. Along the way some interesting features were uncovered. EMPA analyses regions of the sample with lateral dimensions on the order of 1–2 μm and depths of some hundreds of nm [1], [2]. It can provide extremely accurate and precise analysis of these small volumes provided certain conditions are met. This paper discusses variations in analyses of different populations of Y123 and shows that many have marked ranges in oxygen content. The quality of the superconductor strongly depends on its degree of doping [3]. Regions of underdoped Y123 will, therefore, impair the performance of the device and need to be removed. One long-term aim of this research is to correlate spectrometric features of Y123 with transport properties. As will be shown below, the challenges so far encountered in simply generating reproducible and accurate values of spectrometric quantities means that we are not at the stage of attempting any such correlation in this paper and no association with superconducting properties is performed here. This paper is concerned with documenting the steps required to identify regions of different composition and in their accurate analysis.

II. ANALYTICAL TECHNIQUES

The underlying principles and practice of EMPA and WDS are documented in several textbooks (e.g. [1], [2]) and will not be retold here. Several issues important for understanding the difficulties posed in analysis of Y123 are discussed here. In EMPA an electron beam, focused to a probe, interacts with a target that is sufficiently thick to prevent transmission of electrons. An electron in an inner shell of a target atom can be ejected. The resultant transition of another electron to the inner shell produces a characteristic x-ray which may be used to determine the content of the ionized atom in the excitation volume. Deflection of primary electrons by target atoms results in a much larger volume of sample excitation than the diameter of the primary electron probe, depending on the voltage used to accelerate those electrons and on the sample composition. X-rays generated within the target may be absorbed by other atoms in the target. Those with higher energy are more likely to escape the target and so typically sample a greater depth interval than those with lower energy.

Chemical analysis was on a JEOL JXA-8600 microprobe with 15 kV of accelerating voltage and 30 nA beam current. Y was standardized on yttrium aluminum garnet

(YAG: $\text{Y}_3\text{Al}_5\text{O}_{12}$) using the Y $L\alpha$ x-ray, Ba on benitoite ($\text{BaTiSi}_3\text{O}_9$) using the Ba $L\alpha$ x-ray, and Cu and O on Cu_2O using the Cu and O $K\alpha$ x-ray. In each case the peak x-ray count was collected for 100 secs and two backgrounds—one off the peak on each side—for 50 secs each. Monte Carlo analytical models indicate that the depth of sampling falls from 1200 nm for Y to 1100 nm for Ba to 800 nm for Cu to 400 nm for O.

For a single analysis of Y123, the precision of Y content is near 0.8% relative to the nominal 13.5 wt% present; that of Ba is near 0.15% with Ba content = 42 wt%. Cu's nominal 59 wt% is determined with $\approx 0.2\%$ precision. O has a nominal content of 16–17 wt%, determined with a precision of $\approx 0.4\%$.

Textbook interpretations of electronic transitions resulting in x-ray emission treat each atom as if it were in isolation. The nominal assignment for $K\alpha$ x-rays is due to 2p to 1s transitions. In elements heavier than Ne, this assignment is appropriate as 2p and 1s levels are inner shells. In oxides, the 2p electrons of oxygen are in the valence band and so the “2p” O electrons differ in both average energy and in the range of energies in different oxides. The former difference results in a change in energy of the x-ray (difference in energy between initial and final levels) and the latter causes a change in peak shape (height:width). These complications in the analysis of light elements are well known and the normal response has been to synthesize standards of similar chemistry and crystal structure to the unknowns wherever possible [4]. The variable oxygen stoichiometry of Y123 makes this a challenge.

Samples for EMPA mounted in epoxy are polished flat with 1 μm diamond paste and mineral oil lubricant. In most cases the sample is then coated with 25 nm of carbon to make it electrically conductive. Standards are coated with the same thickness of carbon so absorptions of electrons in the primary beam and of emitted x-rays are the same for standards and samples. As discussed below, the process was modified for Y123 analysis. After 1 μm polishing, samples were polished with 300 nm and 50 nm alumina with a mineral oil lubricant. The samples were then ion milled for 2 hours with a Gatan PECS using a 90 μA argon ion beam accelerated through 6 kV. Some samples were carbon coated. In other cases, metal coatings were deposited on the samples using the Gatan PECS with argon ions hitting metal targets to cause sputtering.

Crystallinity of the near-surface region of samples was investigated using electron backscattered diffraction (EBSD) on a JEOL JSM-6330F scanning electron microscope (SEM) equipped with an Oxford ISIS system. Samples were held at 70° to the horizontal so the electron beam strikes the sample at an incidence angle of 20°. The detector is a vertical phosphor screen 20 mm from the sample. For Y123, the Kikuchi pattern is derived from the sample's top ≈ 50 nm [5]. Samples are coated with 15 nm of carbon so that the pattern reflects the crystalline nature of the top ≈ 40 nm of the ceramic.

III. MELTING EXPERIMENTS UNDER RANGE OF $P(\text{O}_2)$

Melting experiments were performed on Y123 at $P(\text{O}_2)$ of 1, 0.1, and 0.01 atm with total $P = 1$ atm (mixed O_2 and Ar). Supersolidus experiments were heated to run temperature,

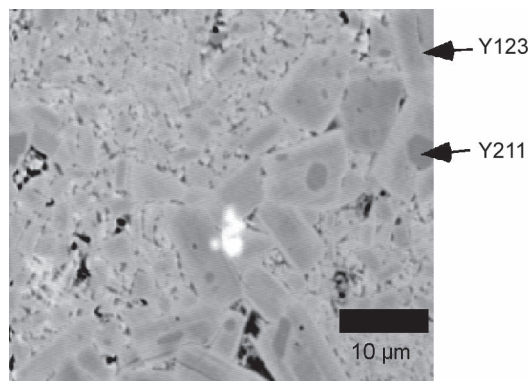


Fig. 1. BSE photomicrograph of Y123 melted at 1018 °C in oxygen at 1 atm and then cooled to 1015 °C over 30 min, held there for one hour and then quenched. The bright area in center is gold derived from suspending loop. Y123 grains each about 10 °C across (many with Y211 cores) form a band from top right to bottom center. Variation in BSE shows Y123 grains are compositionally zoned. Smaller grains in lower right and upper left are similar in BSE intensity to outer parts of large grains. Black areas in the groundmass are copper oxide grains; bright ones are barium cuprate grains.

held for 1 hr, and quenched to Y_2BaCuO_5 (Y211) plus glass. Subsolidus runs were heated 2–5 °C above the solidus for 10 minutes, cooled to subsolidus conditions at 0.1 °C/min and held for 1 hr before quenching. Liquids crystallized to fine mats of Y123 with small amounts of barium cuprate and copper oxide. The solidus was bracketed at between 1015 and 1017 °C in O_2 , between 1001 and 1003 °C at 0.1 atm O_2 , and between 986 and 989 °C at $P(\text{O}_2) = 0.01$ atm. This is a decrease in melting temperature of 15 °C per log unit of $P(\text{O}_2)$ and can be compared with the melting point depression of Bi-2212 of ≈ 30 °C/log $P(\text{O}_2)$ [6]. For melting point decrease, there must be change in activity of a component, at least in the liquid. Cu exists in liquid in both divalent and univalent states as seen in BSCCO [6], [7]. This means that Y123, Y211, and liquid coexist over a temperature interval as the system is ternary not binary. The temperature interval between Y123-absent runs and liquid-absent runs is less than 3 °C, within the precision of experiments.

Fig. 1 is a back-scattered electron (BSE) micrograph of the run product at 1015 °C in pure oxygen. It was heated to 1018 °C and then cooled over 30 minutes to 1015 °C, which is just subsolidus. The very bright area in the center of the view is gold derived from the retaining loop. A band of relatively large (up to 10 μm) crystals of Y123 runs from the upper right corner to the lower part of the micrograph. Many of these have inclusions of Y211. As Y123 grows as a result of reaction of the liquid and Y211 this is not unexpected. At 1018 °C, experimental charges consist of liquid and Y211 crystals similar to inclusions seen here. During subsolidus cooling, Y123 crystals grow on Y211 grains. In many cases Y123 cores are darker than rims, indicating that the former have lower average atomic number than the latter. Several cases in which grains formed from multiple nuclei are denoted by a patchy appearance. Grain size in the lower right and upper left parts of the micrograph is smaller than in this band of larger grains. Zoning in some of these smaller grains may also be seen. The small bright and dark areas are grains of barium cuprate and copper oxide, respectively. These represent the last residual liquids that had

very little yttrium and that mass balance the Y211 for a Y123 bulk composition.

The variation in BSE contrast in these Y123 grains does not reflect huge compositional zoning. The average atomic number of Y211 (assuming stoichiometry) is 22.56. Y123 has values of 22.62 (7 O/formula unit) to 23.83 (6 O/formula unit). A BSE imaging system cannot give actual values of average Z but relative backscattered contrast can be determined. The contrast between brightest and darkest Y123 grains is three times the difference between the darkest Y123 and Y211.

YBCO cation contents in Fig. 1 are near constant (Y211 is $Y_{2.000}Ba_{0.979\pm 6}Cu_{1.096\pm 20}$; Y123 is $Y_{1.000}Ba_{1.911\pm 7}Cu_{3.023\pm 12}$). The variation in Y123 cations is totally inadequate to explain the BSE variation. Oxygen is the only element that can explain the BSE and this encouraged us to improve the quality of oxygen analysis. Moreover, the variation in BSE contrast is consistent with crystallization history if it results from oxygen range. Y123 forms by reaction of Y211 (essentially all Cu is divalent) and $Y_2O_3 - BaO - CuO - Cu_2O$ liquid. Liquid is depleted in Cu(II) relative to Cu(I) as the Cu(II)-rich Y123 forms. Crystallization occurs in less than 30 minutes and the amount of liquid (and its ability to communicate over distances) is decreasing so an equilibrium Cu(II):Cu(I) is not established by oxidation by the surrounding atmosphere. This is fractional crystallization with an element of mixed valence and no external control of $P(O_2)$. Later formed Y123 is starved of oxygen and has lower oxygen content and, therefore, higher average atomic number and backscattered electron intensity.

Analyzed contents of oxygen in Y123 are rather lower than was expected (although Y211 had measured values 99% of expected ones). In pure oxygen the O content per Y atom was 6.3 for darkest cores to 5.5 for lightest rims and ground-mass phases (which are similar in composition). These make nominal valences for Cu 1.88 and 1.47, respectively. Similar results for Y123 were obtained at lower $P(O_2)$ although the range in O contents decreased, primarily at the upper end so the apparent minimum content stayed near 5.5 per Y atom but the maximum was only 5.9 at $P(O_2) = 0.01$ atm. As $P(O_2)$ of synthesis fell and with it the activity of Cu(II) in the liquid, the Cu content of Y123 decreased so that at 0.01 atm O_2 , Y123 averaged $Y_{1.000}Ba_{1.925\pm 9}Cu_{2.861\pm 15}$. There was no obvious complementary change in the composition of Y211 either in Cu or O contents, as it remained near stoichiometry.

Results described above were determined as quickly after experimentation as possible. Samples were taken from the quench cup and set in epoxy. They were polished to 1 μm , immediately coated in carbon and put in the microprobe and held in vacuum until analysis. After analysis, samples were kept in a desiccator for four months and some were reanalyzed without repolishing or carbon coating. None appeared different in electron or optical microscope view from first analysis. There was no difference in cation content from earlier values but oxygen contents had increased to values as high as slightly above 7 oxygen per Y in Y123 analyses. Y211 analyses also showed increase of O content by 10–15%. There is clearly an ageing process that occurs in polished samples.

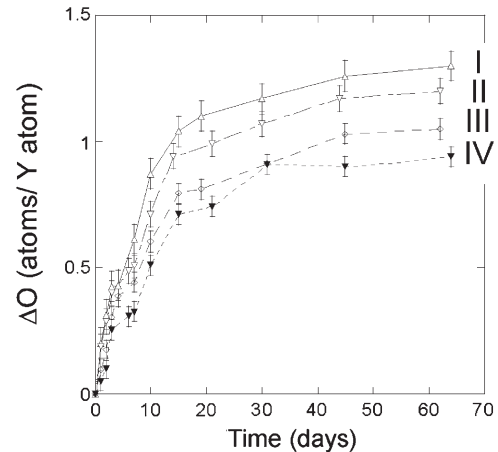


Fig. 2. Ageing of Y123 due to environmental interaction for times up to 2 months. The oxygen content is given as the change in the number of oxygen atoms per Y atom in the analysis. Error bars give general scatter in data. I is population of samples aged in laboratory without carbon coating; II for ageing in a desiccator without carbon coating; III for ageing after carbon coating in laboratory; and IV for ageing after carbon coating in desiccator.

IV. ANALYSIS OF Y123 FROM MELT-TEXTURED MONOLITHS

Investigation of polishing effects on composition needs larger grains than those shown in Fig. 1. Samples cut from one monolithic sample made by top-seeded melt texturing [8] and some ≈ 2 mm thick were broken into pieces. Each was oxygenated for 170 hours at 400 °C in O_2 before mounting in epoxy and polishing before carbon coating. Four room-temperature timed experiments were performed. In the first, samples were exposed to the laboratory atmosphere before carbon coating. In the second, exposure was in a desiccator before carbon coating. In the third, samples were carbon coated and exposed to laboratory air. In the fourth, samples were carbon coated and then exposed in a desiccator (Fig. 2).

Each ageing experiment shows significant O increase. Presumably this is dominated by reaction of Ba in the Y123 with H_2O and then with CO_2 , ultimately to form $BaCO_3$ [9]. No reaction proceeded to the point at which crystals of $BaCO_3$ formed on the Y123 [9], a very obvious feature on a polished surface. Furthermore the amount of O absorbed is much less than expected from carbonation of barium. (Complete replacement of Y123 with Y_2O_3 , CuO, and $BaCO_3$ would give ΔO of about 4; somewhat less if Y211 were in the products.)

The reaction was rapid in the first few days after polishing and then slowed down. It is unsurprising that the reaction was greater when not in a desiccator and with uncoated rather than coated samples. In every case, however, the polished surface accepted extra oxygen over the amount present after polishing.

Although samples reacted with oxygen at temperatures of ≈ 400 °C for periods of a week or more, the first analyses all had 6.2 O atoms/Y atom which is much lower than expected for superconducting Y123 [3]. Further experiments in which portions of the same monolithic YBCO were heated to near solidus temperatures in N_2 and then mounted and polished also gave ≈ 6.2 O atoms/Y atom.

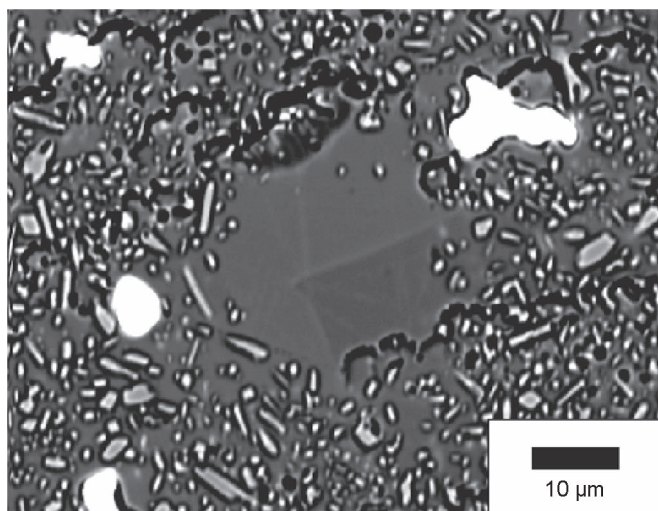


Fig. 3. BSE image of a piece of Y123–Y211 monolith after polishing and ion milling. The bright areas are of metal additives. Y211 grains form sub- μm light grey grains. The matrix is Y123, which is clearly dappled in appearance. The large central patch free from Y211 has bright lines crossing it, but also a bottom right region that is darker (more oxygen) than the rest.

Newly polished YBCO samples were examined by EBSD without obtaining Kikuchi patterns. Samples were then polished to 50 nm and also examined by EBSD with negative results. The samples were then ion milled for 2 hrs, after which strong Kikuchi patterns consistent with the Y123 crystal structure were obtained. Subsequent analysis gave different O contents for samples that had undergone different oxygen treatments. All further discussion of samples is of Y123 that has been polished and ion milled in this manner.

Standard polishing processes produce an amorphous surface layers in which long-range order has been reduced to the extent that electron diffraction does not give a coherent Kikuchi pattern. Destruction of the Y123 structure plausibly means that excess O in the structure is lost so that all the oxygenated Y123 samples produce an amorphous material of similar O content. Polishing could cause reduction or oxidation of copper but the zoning in Fig. 1 suggests that very local patterns are retained. As initial polishing was with 1 μm diamond and the oxygen x-ray signal is from the top 400 nm, it seems likely that the entire O signal is from amorphized material. Even after polishing with 50 nm alumina, the amorphous layer is still $> \approx 40$ nm thick. Two hours of ion milling remove the mirror finish of the sample and reveal grain boundaries and other features of the polycrystalline samples. Analysis of this material is of crystalline Y123 at all depth ranges. The ageing process summarized in Fig. 2 is, therefore, not of crystalline Y123 but of amorphous material.

Despite limited variation in cation composition, BSE images from Y211–Y123 monoliths show significant variation (Fig. 3) although typically on larger scales than in Fig. 1. They are also due to ranges in O of Y123. Therefore, small pieces of one monolith were heat treated: A) O_2 at 412 $^\circ\text{C}$ for 9 days; B) Ar passed through O_2 getter for 21 days at 840 $^\circ\text{C}$; and C) N_2 at 801 $^\circ\text{C}$ for 2 days. Analyses of A are $\text{Y}_{1.000}\text{Ba}_{1.979\pm 10}\text{Cu}_{3.143\pm 14}\text{O}_{6.786\pm 14}$. B are $\text{Y}_{1.000}\text{Ba}_{1.969\pm 10}\text{Cu}_{3.153\pm 14}\text{O}_{6.449\pm 28}$. C has much greater scatter in cations: $\text{Y}_{1.00}\text{Ba}_{1.89\pm 6}$

$\text{Cu}_{2.99\pm 0.09}\text{O}_{6.20\pm 17}$. These heat treatments on small samples apparently reduced the O variation in each portion.

V. COATING WITH MATERIALS OTHER THAN CARBON

Carbon coats of samples offer some protection to the samples from reaction with their environments. We therefore considered coating the samples with metals that might provide even better protection. It is important that the coating layer does not mask the characteristic x-ray signal and does not interfere in the spectrum of interest. Au which presumably could form an inert protective layer on Y123 greatly attenuates the O x-ray signal. A 200 nm Au layer would allow essentially no O x-rays to escape the sample surface. Au also tends to form uneven coats. We have observed in the SEM anomalous portions of Au 20–30 nm thicker than most of the coat. These would cause greatly increased attenuation of the O signal. Furthermore, the presence of Au changes the slope of the background x-rays upon which the O peak rests.

Cr has many positive features as a coat—it attenuates the O K x-ray only about half as much as Au does (although still four times the attenuation of C). It forms smooth even coats. Our analysis of coated materials for Cr x-rays shows a variation only slightly beyond that expected from counting statistics. The presence of Cr raises the background under the O peak somewhat but does so essentially linearly. Analysis of Cr-coated Y123 samples shows, however, rapid increase in O content because of oxidation of the Cr coat. As the oxidation occurs at the very surface of the coat, the resultant O signal is large. Oxidation occurs rapidly so that transferring the sample to the EMPA has a marked influence on the oxygen signal.

Be was ruled out by reason of the acute toxicity of Be. We found no reasonable alternative to carbon coats. Ageing of the Y123 surface was dealt with by milling and recoating samples before analysis if exposed to the environment.

VI. THE SHAPE OF THE OXYGEN X-RAY PEAK

The work before convinced us that we were now at the stage at which we could start to determine the original O content of the YBCO. Another consideration is the standard to be used for O when analyzing YBCO. As discussed before, the O $\text{K}\alpha$ peak is prone to change shape and position from oxide to oxide. We have, therefore, determined the shapes of O peaks in both standards and in different Y123 grains of different O contents to find the best matches between samples and standards.

A. Oxygen X-ray Peaks in Standard Materials

Fig. 4 shows O peak shapes for three potential standard materials. The peaks have been normalized so that both the maximum peak intensity and the low background count rate are the same in each case. The ordinate is therefore intensity without units. The abscissa is the x-ray energy in eV and was calibrated by determining the position of the O $\text{K}\alpha$ peak on $\text{CaMgSi}_2\text{O}_6$ and fixing that as equivalent to 525 eV. Fig. 4 shows replicate analyses of cuprite (Cu_2O), hematite (Fe_2O_3), and yttrium aluminum garnet (YAG; $\text{Y}_3\text{Al}_5\text{O}_{12}$), respectively.

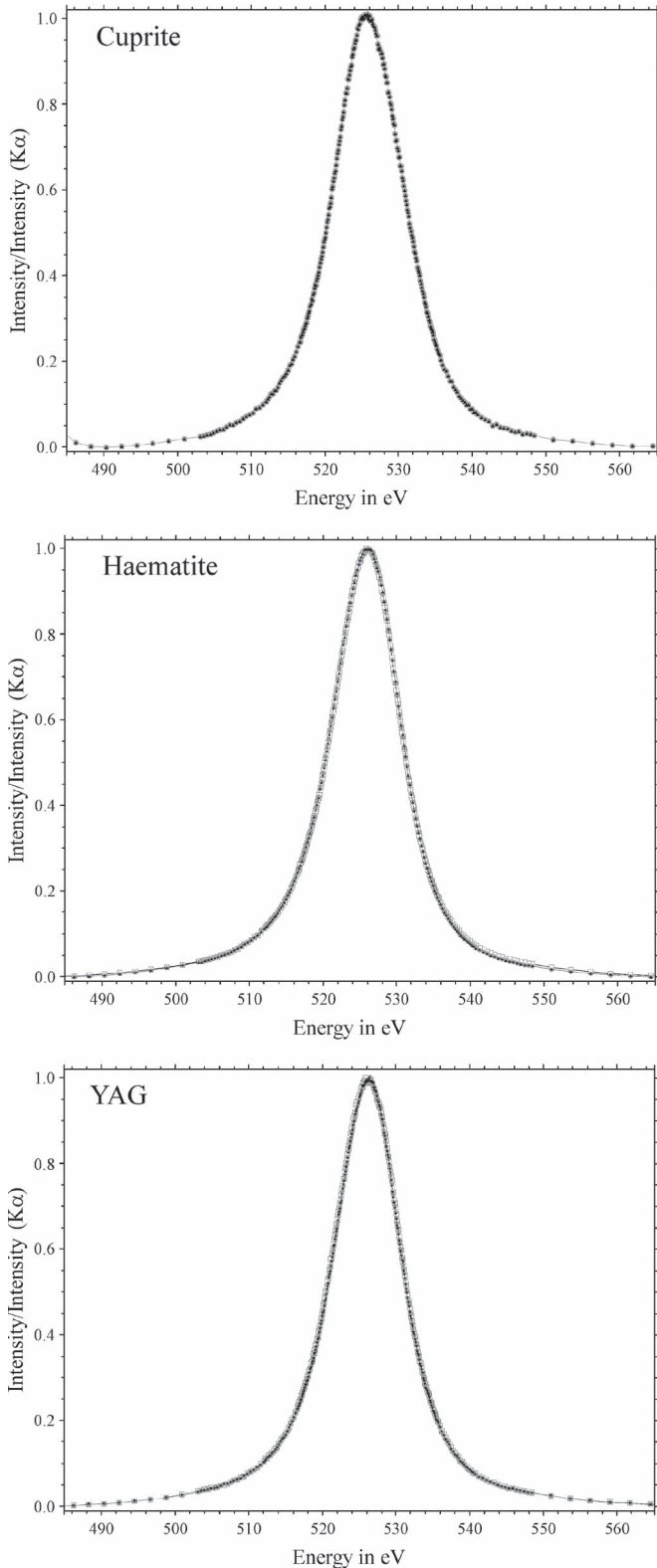


Fig. 4. Replicate scans over oxygen peaks in three materials (cuprite, Cu_2O , hematite, Fe_2O_3 , and YAG—yttrium aluminum garnet— $\text{Y}_3\text{Al}_5\text{O}_{12}$) using 15 kV accelerating voltage and 30 nA beam current. Step size is 0.1 eV and counts were collected for 100 s at each point in the central portion of the peak. These conditions were relaxed for the outer parts of the scans. Scans are normalized so that the maximum in each case is at 1 and the lowest background is at zero. The shapes of the peaks irrespective of the absolute oxygen concentration may, therefore, be compared.

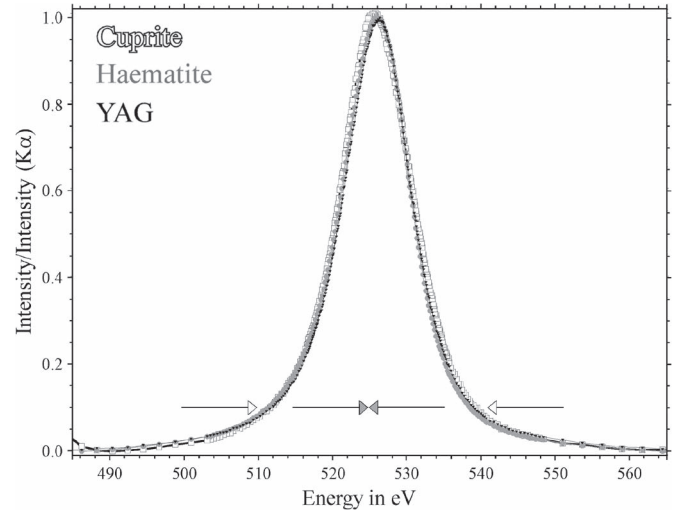


Fig. 5. Comparison of average scans in the three standard materials of Fig. 4. The position of the maxima of cuprite and hematite are clearly offset from that of YAG but the shapes of the peaks appear quite similar. Documentation of differences in peak shape is performed by comparison of positions of the centroid and of the width of the peak at different percentiles of its maximum height. How these values are measured is demonstrated for the 10% percentile: the open-headed arrows indicate the positions of the tails of the peaks; the distance between them gives the width of the peak at that intensity. The average of the values (the position of the two solid arrows) is the centroid at that percentile.

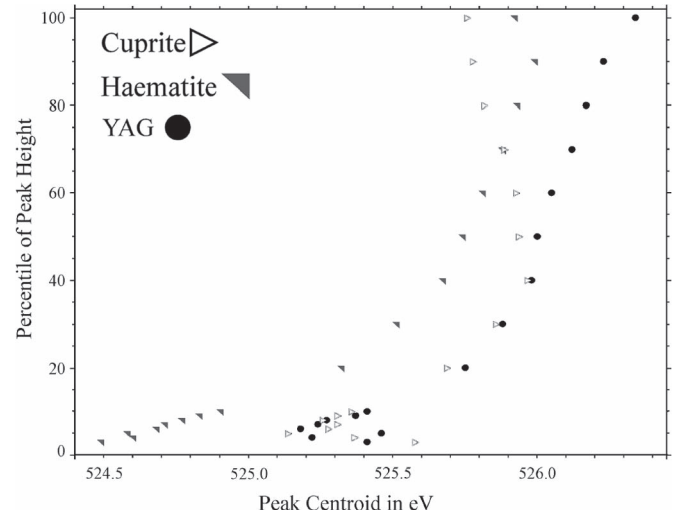


Fig. 6. Changes in the centroids of the oxygen X-ray peaks shown in Fig. 5 with position up the peak. Methodology of determination is shown in Fig. 5. The three standards show differences in their topology as discussed in the text. The relevance of these differences to the quality of chemical analysis is discussed below.

Individual scans agree well with each other. Superposition of the average spectra on each other (Fig. 5) shows some differences between the shapes of the O peaks in the three materials.

Visual examination of peak shape has limited utility in assessing the variability of peak topology. Two simple parameters—center position and width—are used to document differences between these peaks at different percentiles of the maximum peak height (Fig. 5). Fig. 6 shows the change in the centroid of the peaks from near the base to the maximum. Hematite has a relatively smooth curve with systematic shift of

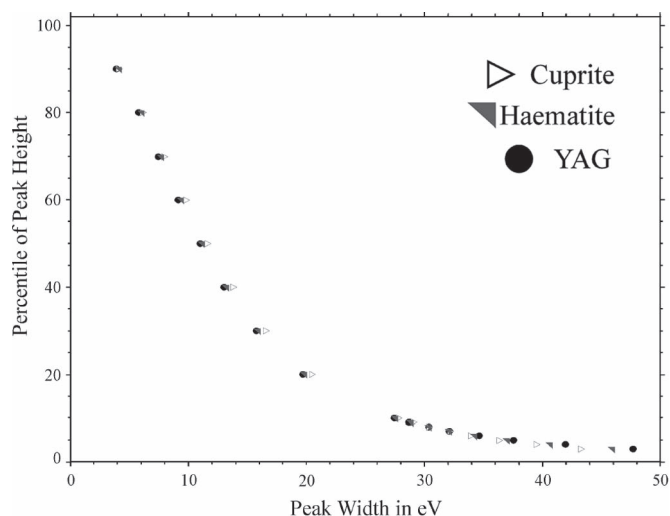


Fig. 7. Changes in the widths of the oxygen X-ray peaks shown in Fig. 5 with position up the peak. Methodology of determination is shown in Fig. 5. Coupled with the data in Fig. 6, these changes document simply the differences in peak topology as discussed in the text.

the centroid to lower energy values on moving down the peak, except that the peak maximum is at somewhat lower energy than the centroid just below the maximum. This is the result of the broader tail of the peak to lower energies than to higher (Fig. 4). The curve for YAG broadly parallels that of hematite despite a kink near 50% height and some scatter in its lower parts. Despite that scatter, the YAG peak is clearly less broad in its lower reaches than is that of hematite. The centroids of the YAG and cuprite peaks are quite similar up to about 50% peak maximum but, whereas there is a slight kink in the YAG curve, the cuprite curve changes slope and moves to lower energy as the intensity increases from 50% to 100%.

The peak widths also show differences in the peak shapes (Fig. 7). Although the widths of the hematite and YAG peaks are quite similar in the higher reaches, YAG has a wider peak in the lower parts so that a greater fraction of the peak area is in the tails of the peak. The cuprite peak shape is quite different—at higher intensities, the cuprite peak is significantly broader than are those of the other oxides but the widths are similar at about 10% of maximum intensity and the cuprite peak is narrower in its tail.

A common approximation made in EMPA is that the peak height at the centroid is a simply related to the area under the peak as it is the latter which depends upon the elemental content. If the differences in peak shape documented in this section do not disrupt this simple relation, then they are irrelevant to analysis of oxygen. One straightforward test to determine the influence of peak topology changes on the quality of the analysis is to determine the oxygen content of each standard relative to the other standards. Thus, analysis of hematite for oxygen using cuprite as standard was performed by standardizing for O on cuprite and for Fe on hematite. The hematite was then analyzed as an unknown using the O peak position determined on cuprite and found to systematically have 0.7% more O than its known content. The position of the O peak was then determined on hematite (a difference of 0.02 eV) and the count rate from cuprite used for comparison. The systematic

error increased to +1.5%. This suggests a slight shift in peak maximum and an O peak in hematite that is taller and narrower (per O content) than in cuprite.

YAG was similarly analyzed for O against cuprite and gave a systematic error of +8.8%. Shifting the position of O analysis to the maximum on YAG rather than cuprite (a shift of 0.48 eV) increases the systematic error to +10.0%. The YAG and cuprite O peaks are, therefore, not only significantly offset from each other but also the former is taller and narrower per unit O content.

Finally, YAG was analyzed against hematite for O and the systematic error was found to be +6.7%. The necessary shift of counting position from hematite to YAG maximum decreased the error to 6.1%. This suggests that, of these three standards, hematite has, relatively, the tallest and narrowest peak. This is consistent with the variations in the shapes of the O peaks of these three standards documented by direct measurement above. It establishes that the amount of peak area enclosed beneath the broad tails of YAG relative to that in the narrower tails of hematite is sufficiently great to induce a systematic error in the analysis that is fifty times the precision of an individual analysis. The greater breadth of the cuprite peak, mostly expressed at higher intensities, induces a systematic error that is two orders of magnitude greater than analytical precision. Clearly the shapes of the x-ray peaks must agree much more closely than those shown in Figs. 4–7 for use of conventional standardization techniques.

The differences between standards, amongst other differences between O peaks, have been monitored on the JXA8600 for over four years and do not change outside analytical precision ($\approx 0.1\%$ relative on each measurement). It is also of note that the common practice of shifting peak position from standard to sample in order to account for the change in the average energy of the electrons associated with the oxygen atom may actually give a greater discrepancy than employing the same peak position in both cases. This is, obviously, because the shape of the O peak (i.e. the range of energy possessed by the relevant electrons) as well as the average energy shows a marked difference between the two phases. Any attempt to “balance” out the deviations by choosing the appropriate peak position to give the desired O content with an obvious misfit of peak shapes is doomed to be well short of a robust solution.

B. Oxygen X-Ray Peaks in Y123

Although the shapes of the peaks in Fig. 4 are similar to each other in appearance at this scale, the differences between them are sufficiently large to generate considerable systematic errors in analysis. Comparison between standards is straightforward as the actual oxygen content of each phase is known and homogeneous. Comparison with Y123 is less easily managed as the actual content of oxygen in the Y123 is unknown. The first step is to determine whether the shape of oxygen scans in Y123 is consistent and whether it shows a general agreement with those in any of our standards.

Fig. 8 shows O scans on several different Y123 bulk and thin film samples, all known to be oxygenated and superconducting. All are very similar at the level displayed in the plots. In

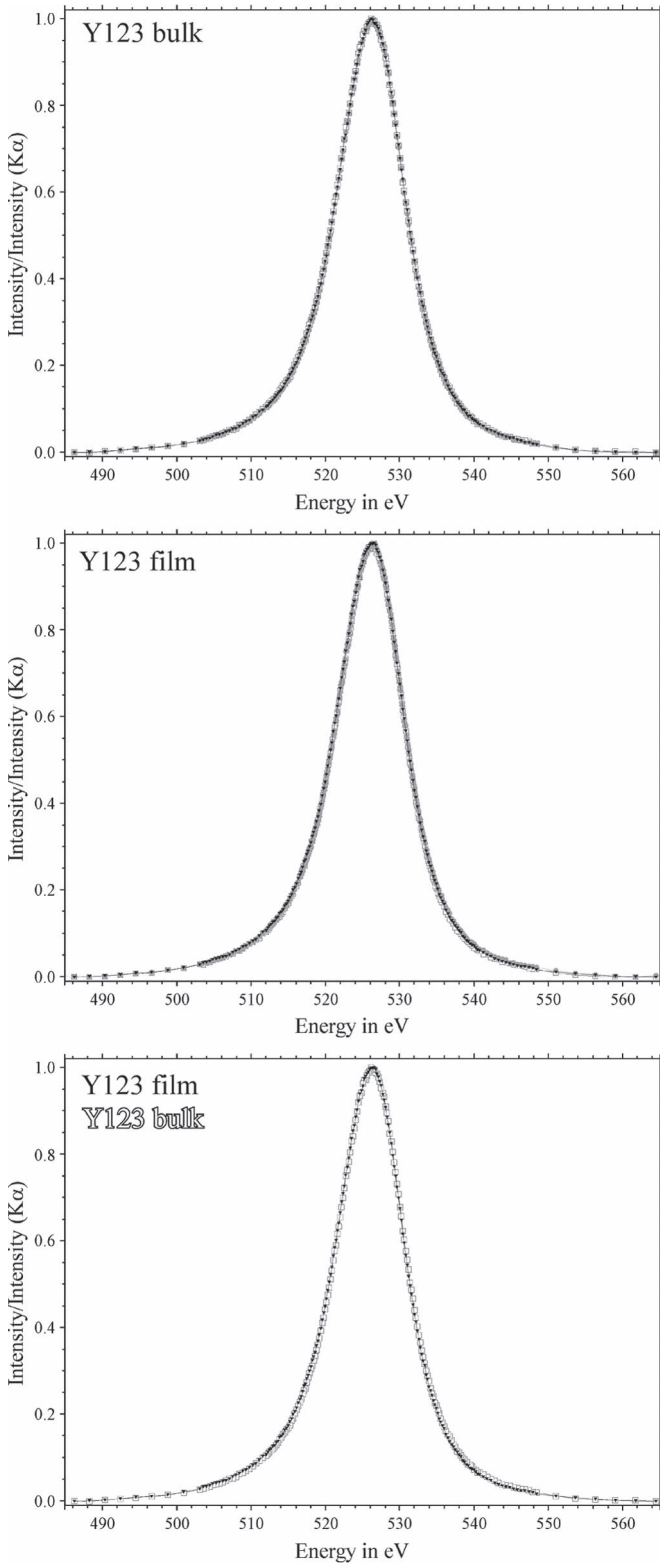


Fig. 8. Replicate scans over oxygen peaks in Y123 bulks and thin films, in each case, oxygenated and superconducting using the same machine and scanning conditions as noted in the caption to Fig. 4, and a comparison of the average of each one. Bulk samples were polished to 50 nm alumina and then ion milled as discussed above; thin films were not processed in any way.

particular, there is no systematic difference between the films (not polished) and the bulk samples (polished and milled). This supports our belief that milling of bulk samples uncovers mate-

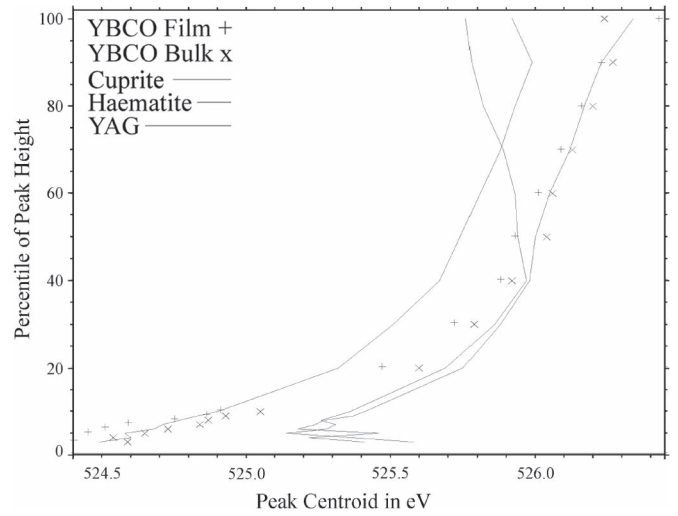


Fig. 9. Centroid variation of oxygen X-ray peak in Y123 bulk and film samples compared with the variations in three standard materials as plotted in Fig. 6. The upper part of the Y123 peaks are similar to that of YAG but gradually diverges with the peak center moving to lower energy values—similar to those of hematite. The difference between the curves exhibited by cuprite and Y123 is marked.

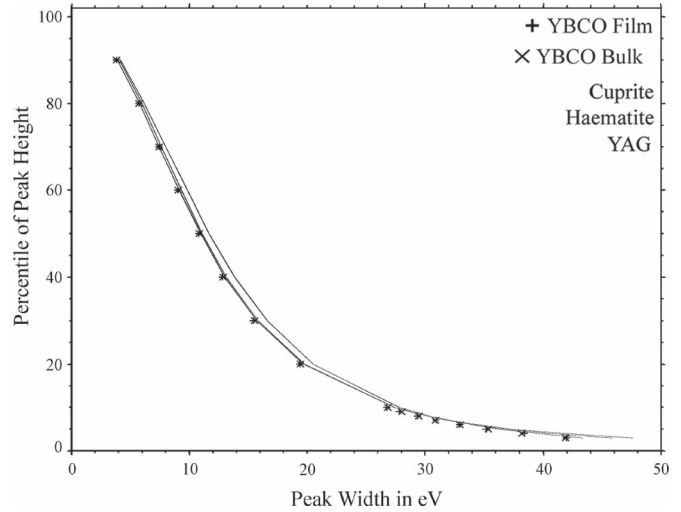


Fig. 10. Peak width variation of oxygen X-ray peak in Y123 bulk and film samples compared with the variation in three standard materials as plotted in Fig. 7. The differences are not as marked in this plot as in Fig. 9, but the Y123 peaks are everywhere somewhat narrower than are those of the standards.

rial in which the electronic state of the oxygen is unaffected by sample preparation and that the milling does not greatly influence the oxygen in the sample.

Figs. 9 and 10 compare centroids and peak widths of O x-ray peaks determined on Y123 film and bulk samples with those determined on the three standards discussed above. As noted above, extreme similarity of the O peak topology between sample and standard are required to avoid the very large systematic errors we observed between different standards.

Variation in peak centroid of the Y123 samples is quite unlike that of any standard (Fig. 9). In addition the peak is systematically narrower than that of a standard (Fig. 10). It is, therefore, unsurprising that Y123 analyses show systematically erroneous analyses for O content in our previous work. This

explains values cited in the early part of the paper which were much lower than expected for superconducting Y123.

The differences in peak topology are most marked between Y123 and cuprite. We successfully employ cuprite as a standard for analysis of many cuprates, including Y211 and, as noted earlier, the oxygen analyses obtained on Y211 in that case are near what is expected by stoichiometry assuming all divalent copper. This raises the possibility that cuprite might be an appropriate standard for non-superconducting Y123. That would indicate that the O x-ray peak in Y123 changes according to the oxygen doping level. At least some of the variation seen for Y123 samples in Figs. 8–10 may, therefore, reflect doping levels and not just be the result of analytical scatter (which should, in any case, be much less than the observed variation based on counting statistics).

All three standards shown have peaks that are relatively wide compared with Y123. That would appear to indicate that the energy range in the electrons in the oxygen valence band in Y123 is smaller than that in any of these standards. Although the width of the oxygen peak is influenced by the range of energies possessed by the “2p” electrons of oxygen, the emission peak is greatly affected by self-absorption of the O x-rays in the sample [10]. Narrow peaks can be generated if the absorption peak moves nearer to the emission peak.

All available high-quality oxygen standards we have used for EPA analysis show O peak shapes distinctly different from that of Y123. This necessitates a new approach to oxygen standardization for Y123 in EMPA, namely curve fitting to the oxygen peak and calculation of the area under the peak. This is an extremely time intensive process which has largely been replaced by an assumption that intensity at the centroid of the peak is a valid measure of area under the peak. Clearly that assumption is not warranted in the case of oxygen in YBCO.

VII. CONCLUSION

At first sight, characterization of Y123 by electron microprobe should be relatively straightforward—and at least no more complicated than is characterization of other ceramic materials. First sight is incorrect. The very act of polishing the sample changes the oxygen content of Y123 from that in the material started with. This is not the case for an unpolished sample viewed in an SEM but there are many other influences on electron emission of an unpolished sample. Normally, scrutiny for heterogeneity by backscattered electron imaging is performed on polished surfaces. In most cases, variability in oxygen content was removed during polishing, presumably because excess oxygen added to the crystal structure in the furnace is removed during amorphization.

Our first BSE image of the monolith shown in Fig. 3 was of a polished surface and the conclusion was that it was near homogeneous. Ion milling of the surface was required to remove the glassy material. While the new surface is depressingly matte and has slight relief (requiring careful situation of analytical points), it does reveal chemical inhomogeneity that was previously obscured. The milling itself may cause damage to the underlying Y123 but the similarity of the oxygen peak shapes

in polished and milled bulk samples and in thin films suggest that the former retain much of the oxygen character they had before sample preparation. Similar issues are not encountered with other ceramics in the Y-Ba-Cu oxide system. Analysis of Y211 using cuprite as oxygen standard gives values of oxygen content near stoichiometry whether the sample is polished or polished and milled. This is consistent with only excess oxygen in Y123 being lost during polishing. That, in turn, suggests that other cuprate superconductors which have excess copper bound in their lattices are likely to lose it during polishing and that ion milling or some other technique needs to be used to remove amorphous layers.

The pattern of inhomogeneity in Fig. 3 is blocky and unlike that expected from diffusion of oxygen into the lattice from grain boundaries and cracks. If, as we believe, the BSE contrast is due entirely to differences in oxygen content, then this material has a range in superconducting properties. In fact this is part of a sample studied elsewhere [11] and shown to have variation in magnitude of trapped charge. Spot analyses of Cu L spectrum and of oxygen content of Y123 in the sample show marked variations across the sample [11]. We now know how to reconcile those results with images of the surface. Further, analyzed oxygen in Y123 in [11] is low for superconducting Y123. The reason for that is now clear.

Analysis of polished surfaces of Y123 (and, probably, of other cuprate superconductors) yields oxygen contents that are correct for the material analyzed—the amorphized surface layer of the Y123—and not representative of the parent material. Ion milling of that amorphized surface uncovers material that plausibly does reflect the composition of the parent material. That, however, remains to be established.

Oxygen analysis by EMPA is very sensitive to small differences in oxygen $K\alpha$ peak shape. That shape is highly dependent upon energy levels occupied by “2p” electrons of oxygen in the ceramic and those levels are, in turn, dependent upon the atomic environment of oxygen. The results show that environments of oxygen in copper oxide, iron oxide, and an yttrium aluminum oxide are sufficiently different as to preclude using those standards to calibrate for analysis of oxygen in another standard. In fact, we have no oxide that has an oxygen peak shape sufficiently close to that of Y123 to permit use of it in the traditional role of calibration.

Future investigations will focus on deriving the entire area of the O $K\alpha$ x-ray peak in order to use that in a more robust standardization. Scans shown above each took, however, 6 hours to acquire; the electron beam has to be very stable for that time. That results in very long analytical times and a more rapid method employing curve fitting is required. The differences between peak shapes are not, however, consistent with the normal curve-shapes of x-ray peaks, suggesting that they are sums of several overlapping peaks, result from self-absorption of the O x-rays in the sample, or both.

ACKNOWLEDGMENT

The authors thank two reviewers and the editor for making them rethink the presentation of data in this paper which has, they hope, greatly improved it from the first draft.

REFERENCES

- [1] S. J. B. Reed, *Electron Microprobe Analysis and Scanning Electron Microscopy in Geology*. Cambridge, U.K.: Cambridge Univ. Press, 1996.
- [2] J. Goldstein, D. E. Newbury, D. C. Joy, C. E. Lyman, P. Echlin, E. Lifshin, L. Sawyer, and J. R. Michael, *Scanning Electron Microscopy and X-Ray Microanalysis*. New York, USA: Springer-Verlag, 2003.
- [3] J. D. Jorgensen, D. G. Hinks, P. G. Radaelli, S. Pei, P. Lightfoot, B. Dabrowski, C. U. Segre, and B. A. Hunter, "Defects, defect ordering, structural coherence and superconductivity in the 123 copper oxides," *Phys. C*, vol. 185–189, pp. 184–189, 1991.
- [4] M. Raudsepp, "Recent advances in the electron-probe microanalysis of minerals for the light elements," *Can. Mineral.*, vol. 33, no. 2, pp. 203–218, Apr. 1995.
- [5] S. X. Ren, E. A. Kenik, K. B. Alexander, and A. Goyal, "Exploring spatial resolution in electron back-scattered diffraction experiments via Monte Carlo simulation," *Microsc. Microanal.*, vol. 4, no. 1, pp. 15–22, Feb. 1998.
- [6] J. K. Meen, V. J. Styve, K. Müller, and C. L. Nguyen, "Phase equilibria in the quinary BSCCO," *IEEE Trans. Appl. Supercond.*, vol. 13, no. 2, pp. 3498–3501, Jun. 2003.
- [7] C. F. Tsang, J. K. Meen, and D. Elthon, "Phase equilibria of the bismuth oxide-copper oxide system in oxygen at 1 atm," *J. Amer. Ceram. Soc.*, vol. 77, no. 12, pp. 3119–3124, Dec. 1994.
- [8] R. L. Meng, L. Gao, P. Gautier-Picard, D. Ramirez, Y. Y. Sun, and C. W. Chu, "Growth and possible size limitation of quality single-grain $\text{YBa}_2\text{Cu}_3\text{O}_7$," *Phys. C*, vol. 232, no. 3, pp. 337–346, Nov. 1994.
- [9] J. P. Zhou and J. T. McDevitt, "Corrosion reactions of yttrium barium copper oxide ($\text{YBa}_2\text{Cu}_3\text{O}_{7-x}$) and thallium barium calcium copper oxide ($\text{Tl}_2\text{Ba}_2\text{Ca}_2\text{Cu}_3\text{O}_{10+x}$) superconductor phases in aqueous environment," *Chem. Mater.*, vol. 4, no. 4, pp. 953–959, 1992.
- [10] C. Bonelle, "Contribution a l'etude des metaux de transition du premier groupe du cuivre et de leurs oxydes par spectroscopie X dans le domaine de 13 Å–22 Å," *Ann. Phys.*, ser. 14 t. 1, pp. 439–481, 1966.
- [11] K. Müller and J. K. Meen, "Cu L-spectra of YBCO, Bi-2212, related cuprates," *IEEE Trans. Appl. Supercond.*, vol. 19, no. 3, pp. 3549–3552, Jun. 2009.